Revista Mexicana de Astronomía y Astrofísica, **53**, 179–188 (2017)

LX LEO: A HIGH MASS-RATIO TOTALLY ECLIPSING W-TYPE W UMA SYSTEM

Birol Gürol[1], Raúl Michel[2], and Chantal Gonzalez[2]

Received August 31 2016; accepted February 21 2017

ABSTRACT

We present the results of our investigation of the geometrical and physical parameters of the binary system LX Leo. Based on CCD BVR_c light curves, and their analyses with the Wilson-Devinney code, new times of minima and light elements have been determined. According to our solution, the system is a high mass-ratio, totally eclipsing, W-type W UMa system. Combining our photometric solution with the empirical relation for W UMa type systems by Dimitrow & Kjurkchieva (2015), we derived the masses and radii of the components to be $M_1 = 0.43M_\odot$, $M_2 = 0.81M_\odot$, $R_1 = 0.58R_\odot$ and $R_2 = 0.77R_\odot$. In addition, the evolutionary condition of the system is discussed.

RESUMEN

Presentamos los resultados de nuestra investigación sobre los parámetros geometricos y físicos del sistema binario LX Leo. En base a curvas de luz, y a su análisis con el código Wilson-Devinney, se han determinado nuevos tiempos de mínimo y los parámetros básicos. De acuerdo a nuestros resultados, el sistema es una variable del tipo W UMa con una tasa de masas grande. Al combinar nuestra solución fotométrica con la relación empírica de Dimitrow & Kjurkchieva (2015), encontramos que las masas y radios de las componentes son $M_1 = 0.43M_\odot$, $M_2 = 0.81M_\odot$, $R_1 = 0.58R_\odot$ y $R_2 = 0.77R_\odot$. Adicionalmente, se discute el estado evolutivo del sistema.

Key Words: binaries: eclipsing — stars: individual (LX Leo) — techniques: photometric

1. INTRODUCTION

LX Leo (ASAS095028+2043.1, CRTS J095027.6+204305, $\alpha_{2000} = 09^h50^m27^s.69$, $\delta_{2000} = +20°43'05''.5$) is a short-period binary system that was discovered during the All Sky Automated Survey (ASAS) and was then classified as a W UMa type eclipsing binary with parameters $V = 12^m.13$, $\Delta m = 0^m.88$, and an ephemeris of $HJD(Min.I) = 2452622.994 + 0^d.235247 \times E$ (Pojmanski et al. 2005) . This system is was also found by the Catalina Sky Survey (Drake et al. 2009). In its associated catalog it was classified as an eclipsing binary with average magnitude, amplitude, and orbital period of $V = 12^m.46$, $\Delta m = 0^m.45$ and $P = 0^d.2352480$, respectively (Drake et al. 2014). According to the all-sky spectrally-matched Tycho2 stars catalog (Pickles & Depagne 2010), the distance to this system is 436 pc. LX Leo can also be found in the UCAC4 (Zacharias et al. 2012) catalog of proper motions (under the name of 554-045545). Its magnitudes in the 2MASS catalog (Skrutskie et al. 2006) are given as $J = 10^m.591 \pm 0.022$, $H = 10^m.081 \pm 0.022$ and $K_s = 9^m.985 \pm 0.02$, and colors $(J - H) = 0^m.510$, $(H - K_s) = 0^m.096$ and $(J - K_s) = 0^m.606$ at the time of observation $JD = 2450836.8873$.

In this work we revise the light elements, within the framework of the well known $(O-C)$ method, using our newly found timings of minimum light along with data found in the literature. Because there is no spectral information available for this system, we use some empirical relations to estimate its geometrical and physical parameters. Finally, its evolutionary status is discussed.

[1]Ankara University, Science Faculty, Dept. of Astronomy and Space Sciences, Turkey.

[2]Instituto de Astronomía, Universidad Nacional Autónoma de México, México.

TABLE 1

$UBV(RI)_C$ AND 2MASS MAGNITUDES OF THE FIELD STARS. IDS AS IN FIGURE 1

ID	Name	RA (2000)	DEC (2000)	U	B	V	R_c	I_c	J	H	K_s
1	LX Leo	147.615528	20.718239	13.581	13.102	12.212	11.678	11.164	10.591	10.081	9.985
2	2MASSJ09501501+2040529	147.562515	20.681321	13.695	13.307	12.466	11.982	11.511	10.787	10.336	10.231
3	2MASSJ09501021+2042218	147.542481	20.706063	13.990	13.978	13.371	12.992	12.639	12.125	11.796	11.733
4	2MASSJ09501054+2046089	147.543870	20.769125	16.724	16.013	15.062	14.488	13.959	13.226	12.699	12.605
5	2MASSJ09502379+2044205	147.599121	20.739021	16.069	15.886	15.143	14.719	14.306	13.738	13.331	13.224
6	2MASSJ09502783+2046222	147.615949	20.772882	18.955	17.762	16.337	15.451	14.564	13.607	12.978	12.768
7	2MASSJ09503319+2045397	147.638310	20.761087	15.547	15.660	15.252	14.991	14.726	14.391	-	-
8	2MASSJ09503741+2043323	147.655932	20.725753	19.327	18.995	17.733	17.225	16.569	15.356	14.721	14.357
9	2MASSJ09503347+2043077	147.639424	20.718858	18.432	17.884	16.977	16.419	15.918	15.246	14.587	14.523
10	2MASSJ09501813+2041421	147.575551	20.695019	17.718	17.022	16.100	15.580	15.124	14.428	13.998	13.796
11	2MASSJ09501015+2041155	147.542298	20.687675	19.371	18.875	17.528	16.960	16.280	14.989	14.282	13.819
12	2MASSJ09501021+2040073	147.542536	20.668759	19.415	19.047	17.674	17.063	16.396	15.134	14.433	13.999
13	2MASSJ09502746+2039505	147.614426	20.664050	19.686	18.424	16.899	15.940	14.509	13.281	12.626	12.376

2. OBSERVATIONS

Photometric observations were carried out at the San Pedro Martir Observatory, on March 22, May 4, and 6, 2016, with the 0.84-m telescope, a filter-wheel and the *Spectral Instruments 1* CCD detector (a deep depletion e2v CCD42-40 chip with gain of 1.39 e^-/ADU and readout noise of 3.54 e^-). The field of view was $7.4' \times 7.4'$ and a binning of 2×2 was used during all the observations. Alternated exposures were taken in filters B, V and R_c with exposure times of 20, 12 and 6 seconds respectively. A total of 931 target images were acquired along with flat field and bias frames.

All images were processed using IRAF[3] routines. Images were bias subtracted and flat field corrected before the instrumental magnitudes of the marked stars in Figure 1 were computed with the standard aperture photometry method. This field was also calibrated in the $UBV(RI)_c$ system and the results, along with the 2MASS magnitudes, are presented in Table 1. Based on this information, we decided to use object #2 as comparison star since it has similar magnitude and color to LX Leo thus making differential extinction corrections negligible. Object #3 was used as check star. Any part of these data can be procured from the authors upon request.

[3]IRAF is distributed by the National Optical Observatories, operated by the Association of Universities for Research in Astronomy, Inc., under cooperative agreement with the National Science Foundation.

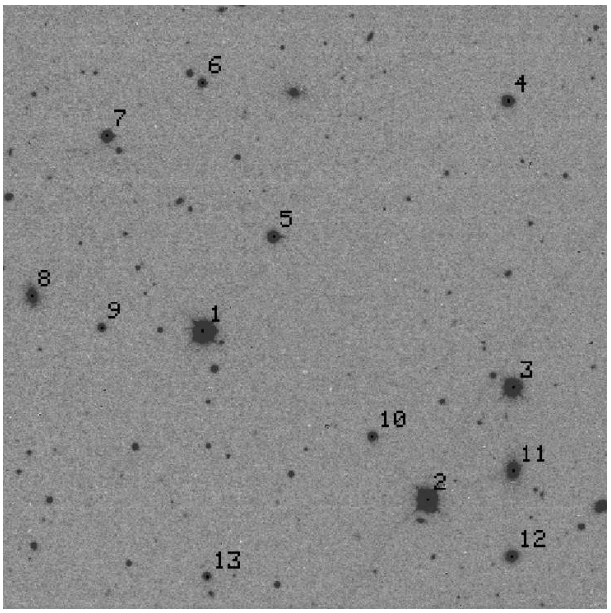

Fig. 1. Observed field. This finding chart was generated by aligning and adding all the images acquired during the second night of observation. The calibrated $UBV(RI)_c$ magnitudes of the marked stars can be found in Table 1.

3. LIGHT ELEMENTS AND $(O-C)$ ANALYSIS

Because the orbital period of LX Leo is important for the rest of the calculations, we tried to refine its value by using our observations and the data found in the literature.

With our observations, and the software package *Minima*25*c* (Nelson 2005), times of light minima were calculated as the error weighted average of the

TABLE 2

OBSERVED TIMES OF MINIMUM

Date	HJD(2400000+)	Error ±	Filter	Type
03.23.2016	57470.74662	0.00004	B	I
	57470.74660	0.00003	V	I
	57470.74648	0.00003	R	I
04.05.2016	57512.73798	0.00005	B	II
	57512.73799	0.00004	V	II
	57512.73806	0.00004	R	II
06.05.2016	57514.73777	0.00003	B	I
	57514.73770	0.00005	V	I
	57514.73777	0.00004	R	I

values found by the different methods implemented. A total of 6 times of primary and 3 of secondary light minima were calculated and are given in Table 2.

Another time of minimum is given by Diethelm (2010) as $HJD(Min.II) = 2455259.8832(2)$ (an ephemeris of $HJD(Min.I) = 2454918.653 + 0^d.235248 \times E$ is also reported). Additionally, we obtained more times of light minima by fitting our theoretical light curves to the ASAS and Catalina Sky Survey data, adjusting simultaneously in magnitude and time. Because of the highly scattered and sparse survey data, these times of light minima are not as good as those in Table 2 and we estimated that their errors are about 0.005 days. Also, by using the light elements by Diethelm (2010), we obtained the $(O-C)$ diagram shown in Figure 2. The small dots correspond to the values obtained by the light curve fitting method. Using these times of light minima, we applied a weighted linear fit to the data getting a revised ephemeris of

$$HJD(Min.I) = 2454918.6560(4) + 0^d.2352482(3) \times E, \quad (1)$$

where the values in parentheses indicate the uncertainty in the last digit, and E is the epoch. This improved ephemeris was used in the rest of the calculations of this study. Because of the limited number of times of minima and the small time spans, we were able to do only a linear fit on the $(O-C)$ variation.

4. PHOTOMETRIC CURVES

In Figure 3, all the observations are plotted with respect to our new light elements.

As can be seen, there is a total eclipse during the primary minimum. The secondary minimum also becomes almost flat except for a small curvature that

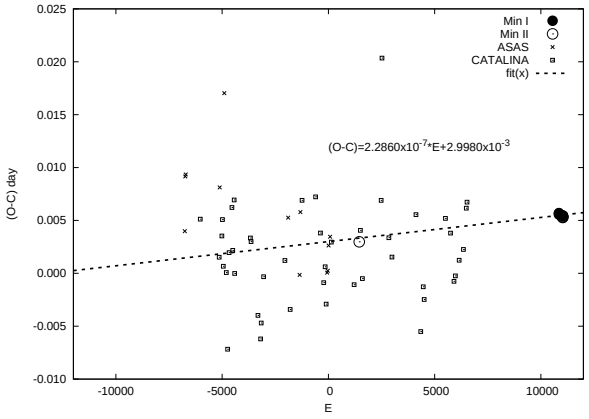

Fig. 2. $(O-C)$ variation of LX Leo.

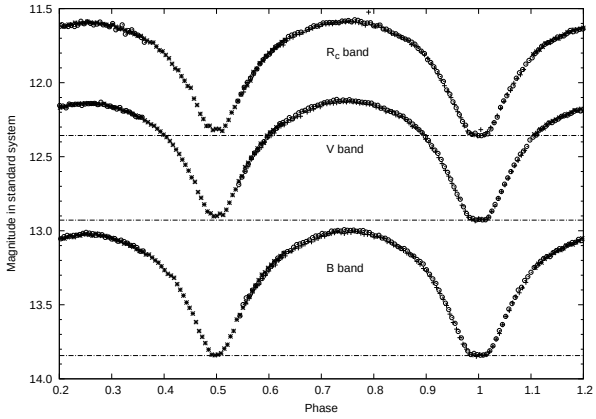

Fig. 3. Phase folded BVR_c light curves of LX Leo. Horizontal lines are plotted to highlight the difference between the minima.

can be attributed to limb darkening of the eclipsed component. For systems which undergo complete eclipse, the derived orbital elements are much more reliable (Binnendijk 1970). Since one of the components is totally eclipsed, we can determine the real magnitudes of the eclipsing and eclipsed components. Additionally, since the depths of the primary and secondary minima are the same for the B filter and only differ slightly for the V and R_c filters, we can say with certainty that the temperatures of the components must be nearly equal. It is important to note that, for light curves that show complete eclipses, the photometric mass ratios are usually very consistent with those obtained spectroscopically (Terrell & Wilson 2005).

The magnitudes at different phases, and the associated colors, are given in Table 3. The difference in depth of the primary and secondary minima is nearly

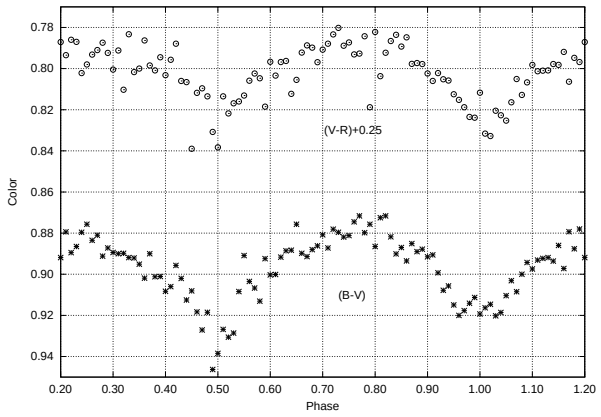

Fig. 4. The observed color curves of LX Leo. The color values correspond to the difference of the averaged magnitudes over 0.01 phase intervals.

zero for the B filter and becomes larger for longer wavelengths. The differences are $0^m.003 \pm 0.009$, $0^m.028 \pm 0.011$ and $0^m.029 \pm 0.016$ for the B, V, and R_c curves, respectively. Furthermore, the primary maximum is lower than the secondary one, the differences being $0^m.021 \pm 0.011$, $0^m.017 \pm 0.007$ and $0^m.010 \pm 0.007$ for the B, V, and R_c curves respectively. This type of variations are due to the O'Connell (1951) effect which can be explained by a hot, or cool, spot on one of the components.

Except during primary minima, most of the W UMa-type systems show small color changes with respect to the orbital phase. It can be seen, Figure 4, that the variations of colors $(B-V)$ and $(V-R_c)$ are no larger than $0^m.04$ and that there is a small color difference between both minima. Because the color $(B-V)$ at the primary minimum is a bit lower than at the secondary minimum, at this phase, we can say that the cooler component is eclipsed by the hotter one. But this is not seen for the $(V-R_c)$ color. If this is true, the cooler component must be larger than the hotter one and the primary minima must show an annular eclipse. Because the color differences between primary and secondary minima are small, $\sim 0^m.024$, it is possible that the eclipsing component at the primary minimum has a hot spot on its surface, making the system bluer during this phase.

We derived the effective temperature of the system from the colors at specific phases. In Table 4 we list the colors and their corresponding temperatures using the color-temperature relations and tables given by Cox (1999), Pecaut & Mamajek (2013), Houdashelt et al. (2000) and Collier et al. (2007). Except for the temperatures obtained for the $(V-R_c)$ color, at primary minimum the hotter component is in front of the cooler one and its mean temperature is 4908 K. The temperatures from JHK colors, which correspond to orbital phase 0.4 when the cooler component is partially in front of the hotter one, imply a mean temperature of 4913 K which agrees with the previous one.

We should expect lower temperatures if the light is highly affected by interstellar reddening but this can not be clearly seen in Table 4. This is possible if the eclipsing system is not far away from us. But if the distance given by Pickles & Depagne (2010) is true, the system must be affected by interstellar dust and gas and, as a result, appear redder at shorter wavelengths. Since the distances of stars determined by Pickles & Depagne (2010) were obtained by using calibrations of absolute magnitudes of single main-sequence stars, they are probably not appropriate for contact binaries. As can be seen in the color curves of Figure 4, the amplitude of the colors does not change more than $0^m.04$ and we can accept that the lower limit of the primary's temperature is around 4900 K.

In principle we do not have any information about the reddening of the system, but it cannot be very large because of the high galactic latitude (+48°). According to the extinction maps[4] of Schlegel et al. (1998), the total extinction in the direction of LX Leo is $A_v = 0.06 - 0.07$. Because these values are given for an infinite distance, the reddening of the system must be smaller. An estimation of reddening can be done, by using total extinction and distance to the system, with the 3rd equation of Bilir et al. (2008). Assuming the distance to the system given by Pickles & Depagne (2010), the resulting reddening is about $0^m.06$, while the corresponding color excess is $E(B-V) = 0.06/3.1 \sim 0.02$.

Additionally, the period-color relation given by Wang (1994) (based on the assumption that the components in a contact binary system are formed from almost normal hydrogen-core-burning stars that obey the mass-radius relation for main sequence stars) predicts that the intrinsic color index can be written as

$$(B-V)_0 = 0.062 - 1.310 \ \log \ P(\text{days}) \qquad (2)$$

where P is the orbital period in days. For this equation, the correlation coefficient to the fit given by Wang (1994) is 0.80. Using the period obtained in this work, we derive the intrinsic color of the system as $(B-V)_0 = 0^m.885$. The color excess obtained

[4] https://ned.ipac.caltech.edu/help/extinction_law_calc.html

TABLE 3

MAGNITUDES AND COLORS OF LX LEO AT DIFFERENT PHASES

Phase	$B \pm \sigma$	$V \pm \sigma$	$R_c \pm \sigma$	$(B-V) \pm \sigma$	$(V-R_c) \pm \sigma$
0.00	13.839 ± 0.007	12.924 ± 0.005	12.347 ± 0.014	0.915 ± 0.009	0.577 ± 0.015
0.25	13.018 ± 0.005	12.141 ± 0.003	11.595 ± 0.006	0.877 ± 0.006	0.546 ± 0.006
0.50	13.835 ± 0.005	12.896 ± 0.009	12.318 ± 0.007	0.939 ± 0.011	0.578 ± 0.012
0.75	12.997 ± 0.010	12.124 ± 0.006	11.586 ± 0.004	0.873 ± 0.011	0.538 ± 0.007

TABLE 4

COLORS AND TEMPERATURES OF LX LEO AT SPECIFIC PHASES

Phase	Color	Cox (1999)	Pecaut & Mamajek (2013)	Houdashelt et al. (2000)	Collier et al. (2007)
	(mag.)	(° K)	(° K)	(° K)	(° K)
0.00	(B-V)=0.915	4821	4995	4909	-
0.00	(V-R_c)=0.577	5329	4764	4774	-
0.40	(H-K)=0.096	4875	-	4812	-
0.40	(J-K)=0.606	4938	-	4937	-
0.40	(J-H)=0.410	4954	-	-	4960

by the difference between the intrinsic and the observed color at phase 0.0 is $E(B-V) = 0.03$ which agrees with the previously obtained value. The corresponding temperatures and spectral types are 4909 K (K1V/K2V) (Cox 1999), 5062 K (K1V/K2V) (Pecaut & Mamajek 2013) and 5053 K (Houdashelt et al. 2000). The average of these temperatures is 5008 ± 86 K and differs by nearly 100 K from the values obtained by using the observed colors. Using the color excess value (~ 0.02) and the $(B-V)$ colors given in Table 3 for different phases, the average temperature is 5073 ± 75 K which is not much different from the previous one. The accepted temperature of the hotter component in the light curve analysis is 5050 ± 100 K.

5. LIGHT CURVE ANALYSIS

Because there is a clear indication of the O'Connell effect, we first want to predict some parameters about the spot, or spots, located on one of the components. For this prediction we fold the first half of the light curves over the second half as shown in Figure 5. As can be seen, around the primary and secondary minima, the spot or spots do not affect the light curves. The variation is mostly seen between phases 0.10 and 0.38 for a cool spot or spots, or between 0.62 and 0.90 for a hot spot or spots. The variation is no larger than $0^m.03$ in the B band and becomes smaller for longer wavelengths. This implies that the spot's temperature factor must be small.

The spot affects $\sim 28\%$ of the light curves. Assuming the spot is located on the equator, its angular radius can be as large as $\sim 50°$. It is also possible that the spot is located away from the equator and can be seen over a large phase interval. Additionally because of the duality between the spot angular radius and temperature factor it is possible that the same effect can be produced with a smaller and hotter spot (or spots). Because of these restrictions the location, angular radius, and temperature factor of the spot (or spots) can only be assumed parameters.

If we assume that the center of the O'Connell effect occurred at orbital phases of 0.24 (for a cool spot) or 0.76 (for a hot spot) we can obtain the longitude of the spot's center as 86°.4 or 273°.6, respectively. Because there is no clear indication of any discrete (pieced) spot structure in this interval, we can say that the effect is most likely produced by a single spot. The activity vanishes at longer wavelengths, especially for R_c where we can hardly see the effect on the light curves (see Figure 7). The fact that the color amplitude decreases towards longer wavelengths suggests that the spot is hotter than the surrounding surface (Kallrath & Milone 1999).

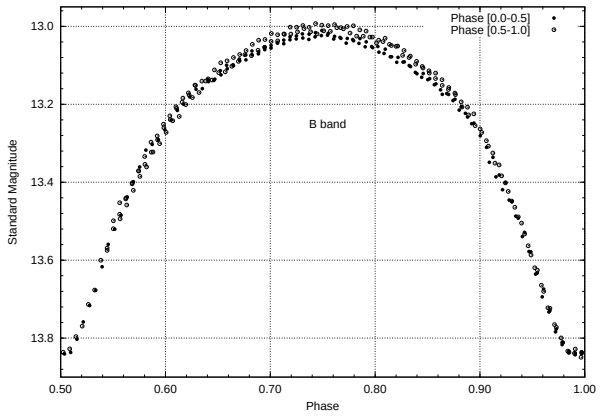

Fig. 5. Folded B light curves of LX Leo with respect to the secondary minima. The O'Connell effect is mostly seen between 0.62 and 0.90 or between 0.10 and 0.38 orbital phases. The effect decreases at longer wavelengths.

The Wilson & Devinney method (Wilson & Devinney 1971; Wilson 1979, 1990; Wilson & van Hamme 2007) was applied to solve the light curves of LX Leo as in our previous paper (Gürol & Michel 2017). The subscripts 1 and 2 refer to the primary (hotter) and the secondary (cooler) component, respectively.

In all our solutions, we have set the temperature of the hotter component to $T_1 = 5050\,\mathrm{K}$ (as obtained in the previous section). The spectral type that matches this temperature is $K1V$ according to the tables by Cox (1999) for main sequence stars. The linear bolometric and logarithmic darkening coefficients were taken from van Hamme (1993). Because of the convective atmospheres, the gravity darkening exponents and the bolometric albedos were set to 0.32 (Lucy 1967) and 0.50 (Rucinski 1969), respectively, for both components. Circular orbit and synchronous rotation were assumed. No third light was allowed for, hence $l_3 = 0.00$. These parameters were kept constant during all the iterations.

For our solutions we assumed that the system is in contact, by employing the Mode 3 option of the code (over-contact mode). The adjustable parameters were: the inclination i, the mean surface temperature of the secondary component T_2, the non-dimensional surface potential of the primary component Ω_1, and the monochromatic luminosity of the primary component L_1. We selected IPB=0; thus, the temperature of the secondary component was used to calculate the L_2 values.

Due to the lack of information on radial velocity, the orbital semi-major axis was estimated using the $P-a$ calibration by Dimitrow & Kjurkchieva (2015); we obtained $a[R_\odot] = 1.72 \pm 0.05$.

Since we see traces of a hot spot on one of the components, we must first obtain a crucial solution using preliminary starting parameters. In order to achieve this, we selected a starting point using a q-mass ratio of 0.5 and we located a hot spot on the secondary component. The spot could also have been located on the primary component but, since the spot modeling is not unique, we simply chose the spot to be on the secondary star as a possible model, and not necessarily the reality. By using the method for modeling such spotted light curves given by Gürol (2005b), who firstly obtained the light curve solution for the unaffected portion of the light curves and then solved the entire light curves by including the spot parameters, we obtained preliminary geometric parameters of the system for the rest of the calculation.

Since no spectroscopic mass ratio and inclination are available, the $[i-q]$-search method was applied for a mass-ratio q ranging from 0.35 to 2.30 and an inclination i ranging from 82°.5 to 90°. We started the $[i-q]$-search by taking i and q constant and setting T_2, Ω, L_1, and the temperature factor of spot as free parameters. The results are given in Figure 6. Mean residuals were defined as the sum of the weighted squared residuals divided by the number of observations (private communication with Wilson, R.E.). As can be seen, the best solution was reached when $i = 87°.5$ and $q_{phot} = 1.90$. This parameters indicate a W-type W UMa system, i.e., the smaller, less massive component has the higher surface temperature but contributes less to the overall brightness of the binary as a whole because the larger star contributes more to the luminosity due to its larger surface area.

By using the initial parameters (T_1, q_{phot}, i and spot parameters) as input values we solved the light curves until the solution converged. The convergent solution was obtained with the adjustable parameters by iterating, until the correction on the parameters became smaller than the corresponding standard deviations. The observed and theoretical light curves, calculated with the final elements, are shown in Figure 7 and the residuals of the fit with the observations in Figure 8. The results of the final solution are given in Table 5 including the standard deviation of the parameters calculated by solving individual light curves. The configuration of LX Leo calculated with the Roche model is shown in Figure 9.

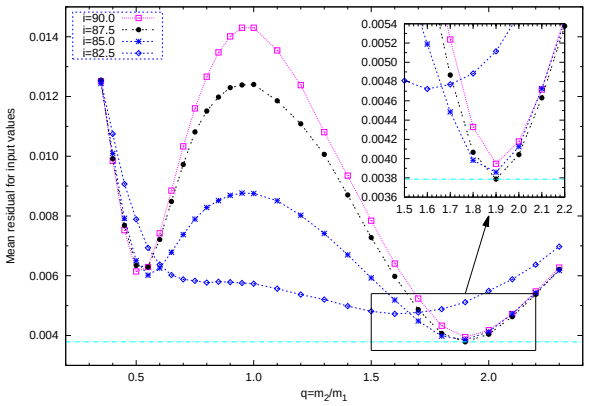

Fig. 6. [i,q] search of LX Leo. Mean residuals for input values as function of the mass ratio and orbital inclination. The $i-q$ search method was implemented by taking i and q as constant and then varying the other parameters, on Mode 3, to find the lowest values of the residuals.

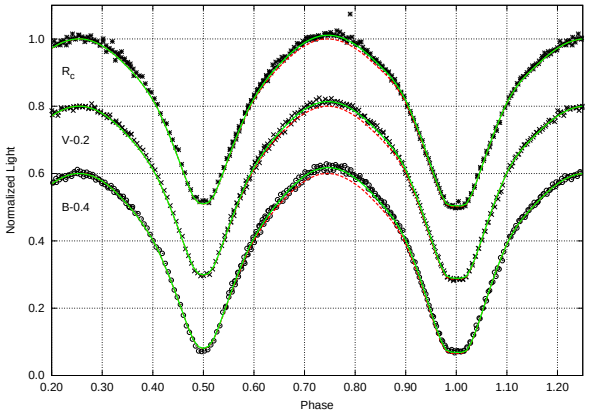

Fig. 7. The observational and theoretical light curves of LX Leo. The symbols represent the observational data for the BVR_c filters and the lines the theoretical light curves for over-contact mode with (continuous) and without (dashed) hot spot located on the secondary component.

6. ABSOLUTE PARAMETERS

Using the semi-major axis of the orbit obtained previously and the orbital period, $P = 0^d.2352482(3)$, we calculated the system's total mass as $1.23 \pm 0.11 M_\odot$. Since the mass ratio of the system was found to be $q = m_2/m_1 = 1.89 \pm 0.02$, we derived the masses of the primary and secondary components as $M_1 = (0.43 \pm 0.04) M_\odot$ and $M_2 = (0.81 \pm 0.07) M_\odot$, respectively.

With the semi-major axis and the mean fractional radii given by the light curve solution we

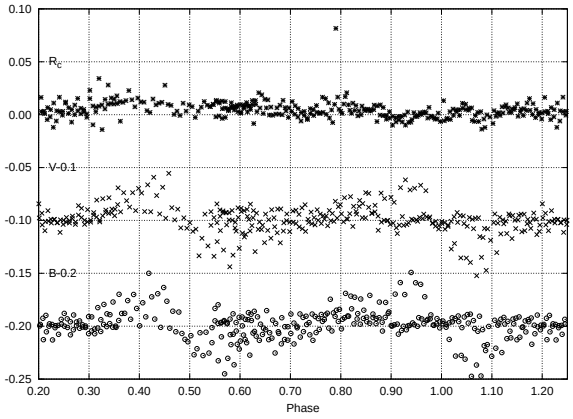

Fig. 8. The residuals of the fit and observed light curves plotted in Figure 7.

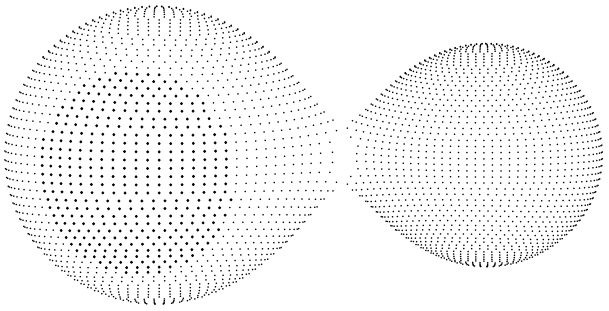

Fig. 9. Roche geometry of the components of LX Leo for the orbital phase 0.75 showing the modeled cool star spot region.

found the radii of the components which are $R_1 = (0.58 \pm 0.02) R_\odot$ and $R_2 = (0.77 \pm 0.02) R_\odot$. Because the sum of the mean fractional radii of the components is $r_{mean} = 0.78 > 0.75$ the system is in a state of marginal contact (Kopal 1959).

Knowing the radii and temperatures of the components, the calculated bolometric magnitudes are $M_{bol1} = 6.54 \pm 0.11$ and $M_{bol2} = 6.03 \pm 0.07$, and the luminosities are $L_1 = (0.19 \pm 0.02) L_\odot$ and $L_2 = (0.31 \pm 0.02) L_\odot$. According to the equations given by Mochnacki (1981), the mean densities of the components are $\rho_1 = 3.16 \pm 0.02$ g cm^{-3} and $\rho_2 = 2.54 \pm 0.02$ g cm^{-3}.

With the period-luminosity-color relation for contact binaries given by Rucinski (2004),

$$M_V = -4.44 \log P + 3.02 (B-V)_0 + 0.12, \qquad (3)$$

we can obtain the absolute magnitude of LX Leo using the orbital period (P in days) and intrinsic color of the system with the error of ± 0.25. By using $(B-V)_0 = 0.877 - 0.02 = 0.857$ and system's orbital

TABLE 5

THE LIGHT CURVE SOLUTIONS OF LX LEO*

Parameter	BVR_c	$\pm\sigma$
$a(R_\odot)$	1.72*	0.05
$i(^\circ)$	86.7	0.6
$q = m_2/m_1$	1.89	0.02
$T_1(K)$	5050*	100*
$T_2(K)$	4916	18
$A_1 = A_2$	0.50*	-
$g_1 = g_2$	0.32*	-
$x_1(bolo)$	0.641*	-
$x_2(bolo)$	0.636*	-
$y_1(bolo)$	0.168*	-
$y_2(bolo)$	0.156*	-
$\Omega_1 = \Omega_2$	4.999	0.026
Ω_{in}	5.089	0.025
Ω_{out}	4.193	0.019
Fillout:$f_1 = f_2$	10.0%	0.4
$L_1/L_{Tot.}(B)$	0.4080	0.0008
(V)	0.3984	0.0007
(R_c)	0.3910	0.0006
$L_2/L_{Tot.}(B)$	0.5920	-
(V)	0.6016	-
(R_c)	0.6090	-
r_1(pole)	0.3125	0.0009
r_1(side)	0.3276	0.0010
r_1(back)	0.3654	0.0011
r_2(pole)	0.4170	0.0007
r_2(side)	0.4440	0.0008
r_2(back)	0.4754	0.0008
σ_B	0.0073**	-
σ_V	0.0067**	-
σ_{Rc}	0.0070**	-
Secondary Component		
Spot co-latitude(°)=	96;	3
Spot longitude(°)=	258;	10
Spot radius(°)=	42.4;	0.7
Spot temp.factor=	1.0079;	0.0010

*Assumed parameters are marked with * and standard deviations for computation of curve-dependent weights with **. The errors given here correspond to the standard deviations of the calculated parameters.

TABLE 6

ABSOLUTE PARAMETERS OF LX LEO

Parameter	Primary	Secondary
Mass ($M_\odot$)	0.43 ± 0.04	0.81 ± 0.07
Radius ($R_\odot$)	0.58 ± 0.02	0.77 ± 0.02
Luminosity ($L_\odot$)	0.19 ± 0.02	0.31 ± 0.02
M_{bol}	6.54 ± 0.11	6.03 ± 0.07
Log g (cgs)	4.55 ± 0.05	4.58 ± 0.05
ρ(g cm^{-3})	3.16 ± 0.02	2.54 ± 0.02
a ($R_\odot$)	1.72 ± 0.05	
d(pc)	207 ± 25	

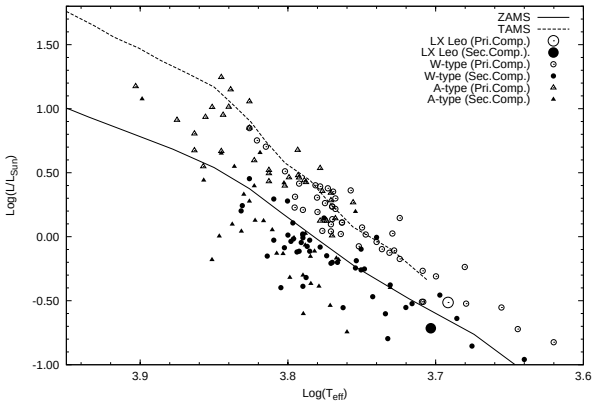

Fig. 10. The location of the components of LX Leo in the $\log T - \log L$ diagram. Open symbols for primary and full symbols denote the secondaries. The sample of W- and A-type systems are from Yakut & Eggleton (2005) and from the works of Gürol et al. (see text). The lines shown are for solar-metallicity, ZAMS (lower) and TAMS (upper) from Girardi et al. (2000).

period, the absolute magnitude of the system turns out to be $M_V = 5.50 \pm 0.25$. Since the V magnitude of the system is 12.141 ± 0.003, we find the distance modulus of the system to be $V - M_V = 6.64 \pm 0.25$ giving a distance to the system of 207 ± 25 pc. In Table 6 we present the absolute parameters of the eclipsing binary system LX Leo. The location of the components of LX Leo on the log $T - \log$ L diagram is given in Figure 10, including other W- and A-type W UMa systems from the list of Yakut & Eggleton (2005) and from the works of Gürol and Gürol et al. (Gürol & Müyesseroğlu 2005a; Gürol 2005b; Gürol et al. 2011a,b, 2015a,b,c, 2016a; Gürol 2016b; Gürol & Michel 2017). As can be seen, the primary component is located within the main-sequence while the secondary component is located below it, consistent with the other W-type systems.

7. RESULTS AND DISCUSSION

We have derived, for the first time, a photometric solution for the eclipsing binary system LX Leo. We found that this binary is a W-type over-contact system with a mass ratio of $q = 1.89 \pm 0.02$, and a shallow degree of physical contact ($f = (\Omega_{in} - \Omega)/(\Omega_{in} - \Omega_{out}) = 10\%$) including thermal contact between components ($\Delta T \sim 134$K). The photometric mass ratio found in this work can only be confirmed by spectroscopic observations, but as can be seen in several works (Lapasset 1992; Maceroni and van't Veer 1996; Terrell & Wilson 2005) the photometric and spectroscopic mass ratios are very consistent with each other for W UMa type systems showing total eclipse.

Because of restricted time span of times of light minima we cannot say much about the period variation of the system, but with the available data we refined the light elements and used them in this analysis. We found that the light curves showed a decreasing O'Connell effect toward longer wavelengths, which we assume is produced by a hot spot located on the secondary component with a small temperature factor. The corresponding spectral types for the components are approximately $K0V + K1V$ for the primary and secondary, respectively.

Absolute parameters were obtained by using the empirical relation given for W UMa type systems by Dimitrow & Kjurkchieva (2015); the uncertainties of the parameters are relatively small.

Overcontact systems are important objects in astrophysics, especially for understanding the very late evolutionary stages of the binaries connected with the processes of mass and angular momentum loss, merging or fusion of the stars, etc.

RM acknowledges financial support from the UNAM under DGAPA grant PAPIIT IN 105115. This paper is based on observations acquired at the OAN-SPM, Baja California, Mexico. This research has made use of the SIMBAD database, operated by CDS, Strasbourg, France, and NASA's Astrophysics Data System Abstract Service. This publication makes use of data products from the Two Micron All Sky Survey, which is a joint project of the University of Massachusetts and the Infrared Processing and Analysis Center/California Institute of Technology, funded by the National Aeronautics and Space Administration and the National Science Foundation. We would like to thank the anonymous referee for all his/her very useful comments and corrections which improved the quality of this paper.

REFERENCES

Bilir, S., Ak, T., Soydugan, E., et al. 2008, AN, 329, 835
Binnendijk, L. 1970, VA, 12 (1), 217
Collier C. A., Wilson, D. M., West, R. G., et al. 2007, MNRAS, 380, 1230
Cox, Arthur N. (ed.) 1999, Allen's Astrophysical Quantities, fourth ed. Springer-Verlag
Diethelm, R. 2010, IBVS, 5945
Dimitrov, D. P. & Kjurkchieva, D. P. 2015, MNRAS, 448, 2890
Drake, A. J., Djorgovski, S. G., Mahabal, A., et al. 2009, ApJ, 696, 870
Drake, A. J., Graham, M. J., Djorgovski, S. G., et al. 2014, ApJS, 213, 9
Girardi, L., Bressan, A., Bertelli, G., & Chiosi, C. 2000, A&AS, 141, 371
Gürol, B. 2005, NewA, 10, 653
_____. 2016, NewA, 47, 57
Gürol, B., Bradstreet, D. H., Demircan, Y., & Gürsoytrak, S. H. 2015, NewA, 41, 26
Gürol, B., Bradstreet, D. H., & Okan, A. 2015, NewA, 36, 100
Gürol, B., Derman, E., Saguner, T., et al. 2011, NewA, 16, 242
Gürol, B., Gökay, G., Saral, G., et al. 2016, NewA, 46, 31
Gürol, B., Gürsoytrak, S. H., & Bradstreet, D. H. 2015, NewA, 39, 9
Gürol, B. & Michel R. 2017, NewA, 51, 128
Gürol, B. & Müyesseroğlu, Z. 2005, AN, 326, 43
Gürol, B., Terzioğlu, Z., Gürsoytrak, S. H., Gökay, G., & Derman, E. 2011, AN, 332, 690
Houdashelt, M. L., Bell R. A., & Sweigart A. V. 2000, AJ, 119, 1448
Kallrath J. & Milone, E. F. 1999, Eclipsing Binary Stars (New York, NY: Springer-Verlag)
Kopal Z. 1959, Close Binary Systems (London, Chapman & Hall)
Lapasset, E., Gómez, M., & Farinas, R. 1992. IAU 151, Evolutionary Processes in Interacting Binary Stars, ed. Y. Kondo, R. F. Sistero, & R. S. Polidan (Boston, MA: IAU), 387
Lucy, L. B., 1967, ZA, 65, 89
Maceroni, C. & van't Veer, F. 1996, A&A, 311, 523
Mochnacki, S. W. 1981, ApJ, 245, 650
Nelson, R. H. 2005. Software by Bob Nelson, `http://members.shaw.co/bob.nelson/software1.htm`
O'Connell, D. J. K. 1951, PRCO, 2, 85
Pecaut, M. J. & Mamajek, E. E. 2013, ApJS, 208, 9
Pojmanski, G., Pilecki, B., & Szczygiel, D. 2005, AcA, 55, 275
Pickles, A. & Depagne, E. 2010, PASP, 122, 1437
Rucinski, S. M. 1969, AcA, 19, 245
_____. 2004, NewAR, 48, 703
Skrutskie, M. F., Cutri, R. M., Stiening, R., et al. 2006, AJ, 131, 1163
Schlegel, D. J., Finkbeiner, D. P., & Davis, M. 1998, ApJ, 500, 525

Terrell, D. & Wilson, R. E. 2005. Ap&SS, 296, 221
van Hamme, W. 1993, AJ, 106, 2096
Wang, J. M. 1994, ApJ, 434, 277
Wilson R. E. 1979, ApJ, 234, 1054
_____. 1990, ApJ 256, 613
Wilson R. E. & Devinney, E. J. 1971, ApJ, 166, 605
Wilson R. E. & van Hamme W. 2007, Documentation of Eclipsing Binary Compute Model, Astronomy Department, University of Florida, Gainesville
Yakut, K. & Eggleton, P. P. 2005, ApJ, 629, 1055
Zacharias, N., Finch, C. T., Girard, T. M., et al. 2012, The fourth U.S. Naval Observatory CCD Astrograph Catalog (UCAC4)

C. Gonzalez: Universidad Nacional Autónoma de México. Observatorio Astronómico Nacional. Apartado Postal 877, C.P. 22800, Ensenada, B. C., México (chantal@astro.unam.mx).
B. Gürol: Ankara University, Science Faculty, Dept. of Astronomy and Space Sciences, 06100 Tandoğan, Ankara, Turkey (Birol.Gurol@ankara.edu.tr).
R. Michel: Universidad Nacional Autónoma de México. Observatorio Astronómico Nacional. Apartado Postal 877, C.P. 22800, Ensenada, B. C., México (rmm@astro.unam.mx).